Polymer Chemistry

ROYAL SOCIETY OF CHEMISTRY

PAPER

View Article Online
View Journal

Cite this: DOI: 10.1039/d6py00299d

Stereocontrol as a tool for shaping abiotic, sequence-defined oligourethanes

Sara Njoku,†[a] Ariel F. Perez Mellor, †[b] Johanna Brazard, [b] Simone G. Giuffrida, [a] Wojciech Dudziak, [c] Céline Besnard, [d] Thomas Bürgi, [b] Takuji B. M. Adachi *[b] and Róża Szweda *[a,c]

Received 26th March 2026,
Accepted 6th May 2026

DOI: 10.1039/d6py00299d

rsc.li/polymers

Nature leverages the primary sequence of proteins to guide the folding of protein chains into specific three-dimensional shapes, which are crucial for their function. Similarly, abiotic polymers can be engineered with a precise arrangement of monomers and stereocenters through multistep iterative synthesis. This study explores experimental and computational methods to examine the folding of model oligourethanes and how stereochemistry can tune secondary structures. Our findings reveal that isotactic oligourethanes can form helical conformation in non-polar aprotic media. The sequence of stereocenters in the polymer backbone fine-tunes the resulting secondary structures and shifts from helical to zig-zag shapes. While extensive research has focused on amide-based backbones due to their similarity to proteins, we demonstrate how to fold urethane-based structures that could be a foundation for developing non-biological polymers with protein-like features. The shape control of oligourethanes is crucial for their envisioned functions, such as catalytic activity and intramolecular interactions with ligands, making stereocontrol a powerful tool for the advanced engineering of polymer properties.

Introduction

Nature has achieved a remarkable level of fine-tuning the functionality of proteins through their controlled structure, which is still beyond the reach of abiotic macromolecules.[1] The information encoded by the sequence of amino acids in the protein polyamide chain dictates the formation of the secondary structure and, subsequently, the specific role of the protein. Nowadays, similarly to natural proteins, abiotic polymer backbones can be fabricated, preserving the defined order of monomers using multistep iterative synthesis.[2–5] Moreover, the use of chiral monomers enables precise stereocontrol of the backbone.[6] Among these, we can find examples of oligo (urethane-amide)s,[7] oligotriazoles,[8–10] poly(thioether-amide)s,[11] polyesters,[12] and oligourethanes.[13,14] In other words, non-natural macromolecules can be synthesized with a controlled primary structure. Building on these developments, including our prior work demonstrating the controlled synthesis of stereo-defined oligourethanes[13,14] it becomes increasingly important to understand how monomer sequence and stereochemistry govern folding and secondary structure in abiotic polymers. Such insight is essential for establishing design rules that translate primary structure into predictable higher-order organization and ultimately function.

Classical polymers in solution typically adopt "random coil" conformations.[15] However, these conformations can be controlled by tailoring polymer primary structure, including sequence, chain length, and stereochemistry or tacticity.[16] Achieving precise control over polymer conformations in solution remains challenging and requires directional secondary interactions at the single-chain level.[17–23] Inspired by natural systems, foldamers, sequence-specific oligomers,[24] have been developed to achieve well-defined 3D shapes directed by strong directional interactions and rigidity of backbones.[25–28] While extensive research has focused on amide-based backbones,[29] including peptoids,[30,31] due to their similarity to proteins, the folding behavior of non-amide-based structures remains largely unexplored,[32–34] especially in organic solvents distinct from physiological environments.

Harnessing secondary structure control in organic solvents offers a powerful route to designing synthetic macromolecules with precise, programmable functions, unlocking new possibilities in selective catalysis, molecular sensing, and other high-performance applications. Despite remarkable advances in fol-

[a]Łukasiewicz Research Network – PORT Polish Center for Technology Development, Stabłowicka 147, 54-066 Wrocław, Poland
[b]Department of Physical Chemistry, Sciences II, University of Geneva, 1211 Geneva, Switzerland. E-mail: Takuji.Adachi@unige.ch
[c]Center for Advanced Technologies, Adam Mickiewicz University, Uniwersytetu Poznańskiego 10, 61-614 Poznań, Poland. E-mail: roza.szweda@amu.edu.pl
[d]Laboratory of crystallography, University of Geneva, 1211 Geneva, Switzerland
†Authors contributed equally.

damer design, key challenges remain in translating structural control into real-world applications.[35,36] Achieving complex tertiary architectures with protein-like sophistication[37–39] that can rival enzymes or receptors, and create therapeutically relevant scaffolds for drug discovery[40] represent major frontiers. At the same time, practical hurdles such as scalable synthesis, cost-effectiveness, and integration with high-throughput or evolutionary approaches must be overcome to unlock the full potential. Therefore, developing foldamers on non-amide backbones, such as polyurethanes, which can be fabricated on a large scale and extended to relatively long chains,[41] is particularly important. Exploring different abiotic polymer backbones can extend the operational window of traditional foldamers and open access to media previously restricted by solubility limitations, for instance, conditions highly relevant for organic catalysis and molecular recognition, which form the foundation for designing advanced, functional materials.

In this work, we demonstrate that oligourethanes can fold into different well-defined secondary structures tunable by the stereochemistry of the monomer units in non-aqueous solution. Combining experimental and theoretical methods, we show that short tetramers with varying sequences of stereocenters are prone to attain conformations of distinct shapes in non-polar media. Specifically, the isotactic *SSSS* sequence, where *S* denotes the absolute stereoconfiguration of the monomer units, folds into a helical structure, while replacing *S* with *R* units in an alternating manner introduces disorder in the helix, resulting in an elongated, sheet-like structure. The presented study is an initial step to gain complete control over polyurethane secondary structures that can mimic protein features and finally be designed to display specific functionalities.

Results and discussion

Design, synthesis and characterization of oligourethane library

Four sets of abiotic oligourethanes with a defined sequence of stereocenters were synthesized to investigate folding and the impact of stereochemistry on the resulting secondary structures (Fig. 1). To introduce entropic constraints and promote the formation of well-defined secondary structures, we have chosen (*R*)- and (*S*)-enantiomers of chiral 2-aminopropan-1-ol as the monomeric building blocks. This way, we limited the distance between urethane bonds to two carbon atoms while designing synthetically accessible structures. Each monomeric unit has a stereogenic center located at the carbon adjacent to the nitrogen atom of the urethane group. As we previously reported, substituting 3-aminopropan-1-ol monomers,[42] having three carbon atoms between urethane groups, with their constitutional isomer 2-aminopropan-1-ol resulted in a significant increase of the backbone rigidity, as evidenced by the increase in the T_g values.[14,43] On the other hand, the urethane group adopts a stable planar conformation due to the delocalization of π-electrons on the backbones, which can be further stabilized by intra-chain hydrogen bonds, as reported for monomer[44] and oligourethane-ligand complexes.[45] Therefore, we hypothesized that oligourethanes constructed from chiral 2-aminopropan-1-ol monomers can form stable secondary structures that can be tuned by a sequence of stereocenters. To test the hypothesis, we investigated the three-dimensional structure of model oligourethanes by Density Functional Theory (DFT) and several experimental methods in chloroform, representing non-polar, aprotic media. Oligourethanes with a defined sequence of stereocenters are obtained by multistep solution synthesis that involves two iterative steps: (i) activation of a hydroxyl group by *N*,*N*-disuccinimidyl carbonate (dSu) and (ii) chemoselective coupling of amino alcohol monomer followed by aqueous washing (Fig. 1a, Scheme S1 and Tables S1–S3).[14] For characterization of obtained oligourethanes see SI (Fig. S1–S28).

The synthesized library of oligourethane tetramers varies in the number (O1, O2, O4) and arrangement (O2, O3) of *S* and *R* stereocenters, which influence their thermal characteristics. Differential Scanning Calorimetry (DSC) analyses (Fig. 2a and S29) reveal that the stereocenter sequence significantly influences intermolecular interactions, as reflected in different T_m values and crystalline properties among diastereoisomers in the solid state. The T_m obtained from the first heating curve for the isotactic sequence is T_m = 130 °C, and the change in stereochemistry of the last monomer unit leading to the sequence *SSSR* does not cause a significant difference. A drastic change is observed when the stereocenter of the second monomer is altered), leading to an increase of about 17 °C in T_m, up to 147 °C for **O3** ***SRSS***. Change of stereochemistry into an alternated manner in **O4** ***SRSR***, where the second and the last monomers are turned to opposite stereoconfiguration, leads to an even further increase in T_m up to 167 °C, which is 37 °C higher compared with the isotactic motif. The same behavior was observed for enantiomer series O1′–O4′ (Fig. S29). From the second heating curves, we can clearly see that T_g, which represents backbone rigidity, occurs at about 40 °C and remains unchanged across all investigated sequences. The two sequences, O3 and O4, exhibit highly crystalline properties that enable further examination in the solid state using X-ray crystallography for O3 and 3D electron diffraction for O4. Interestingly, the DSC data correlate with the distinct crystal structures of the studied diastereoisomer series. The **O3** ***SRSS*** and **O4** ***SRSR*** in the solid state form flat, zig-zag-shaped structures that promote orderly chain packing, leading to a conformational arrangement resembling a sheet-like structure (Fig. 2b and S30–S33). For **O1** ***SSSS*** and **O2** ***SSSR***, however, suitable crystals for structural analyses have not been obtained so far.

Computational studies of the oligourethane conformation landscape

Structural differences in solution among oligourethanes were revealed by theoretical explorations of the conformational landscape of each oligomer using DFT. Depending on the sequence of stereocenters, the calculated secondary structure of O1–O4 is indeed different, as visualized in Fig. 3a. **O1** ***SSSS*** shows an ordered helical conformation, whereas **O4** ***SRSR*** is

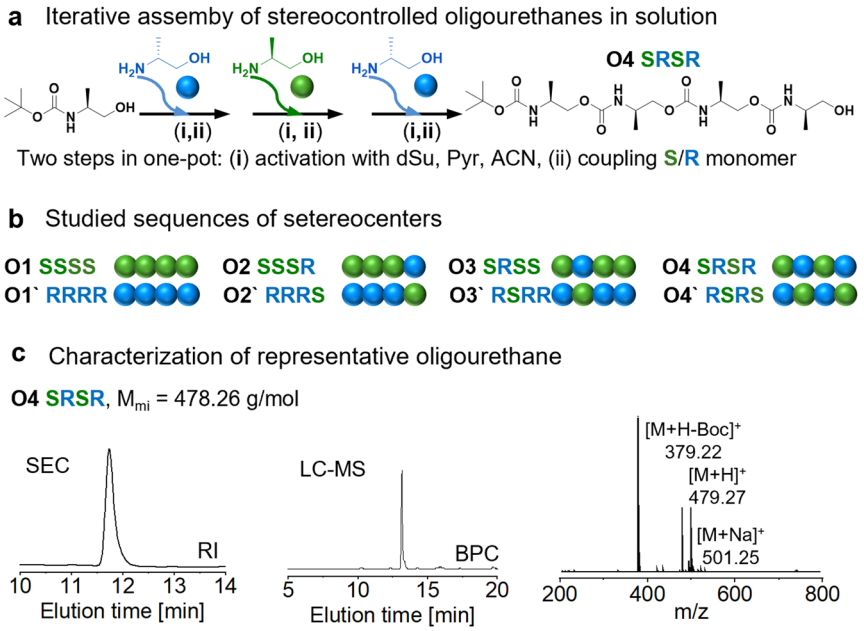

Fig. 1 (a) Synthesis route to oligourethanes. (b) A library of investigated oligourethanes O1–O4 and their enantiomers O1′–O4′. (c) Characterization of representative oligomer **O4** ***SRSR*** by Size Exclusion Chromatography (SEC, refractive index – RI trace) and Liquid Chromatography – Mass Spectrometry (LC-MS, base peak chromatogram – BPC trace); for others, see Fig. S1–S28.

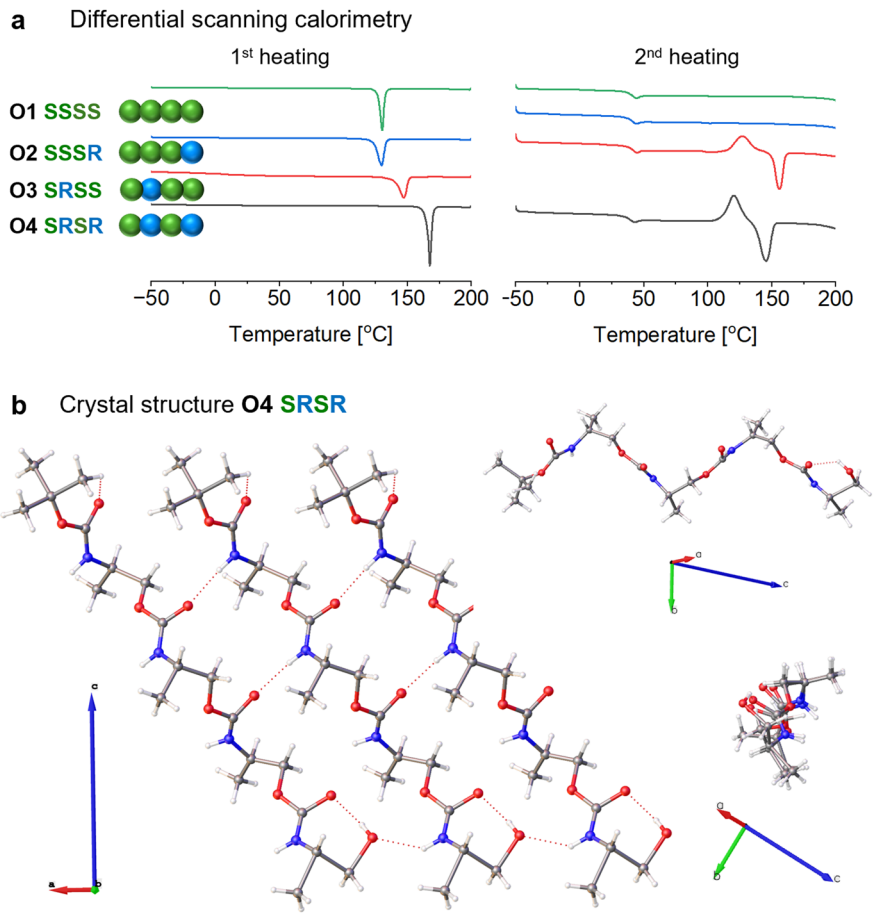

Fig. 2 (a) Differential scanning calorimetry analyses of O1–O4 oligourethanes. (b) Crystal structure of O4 oligourethane "top view", "side view" and packing (coordinate systems indicated). For O3, see Fig. S30.

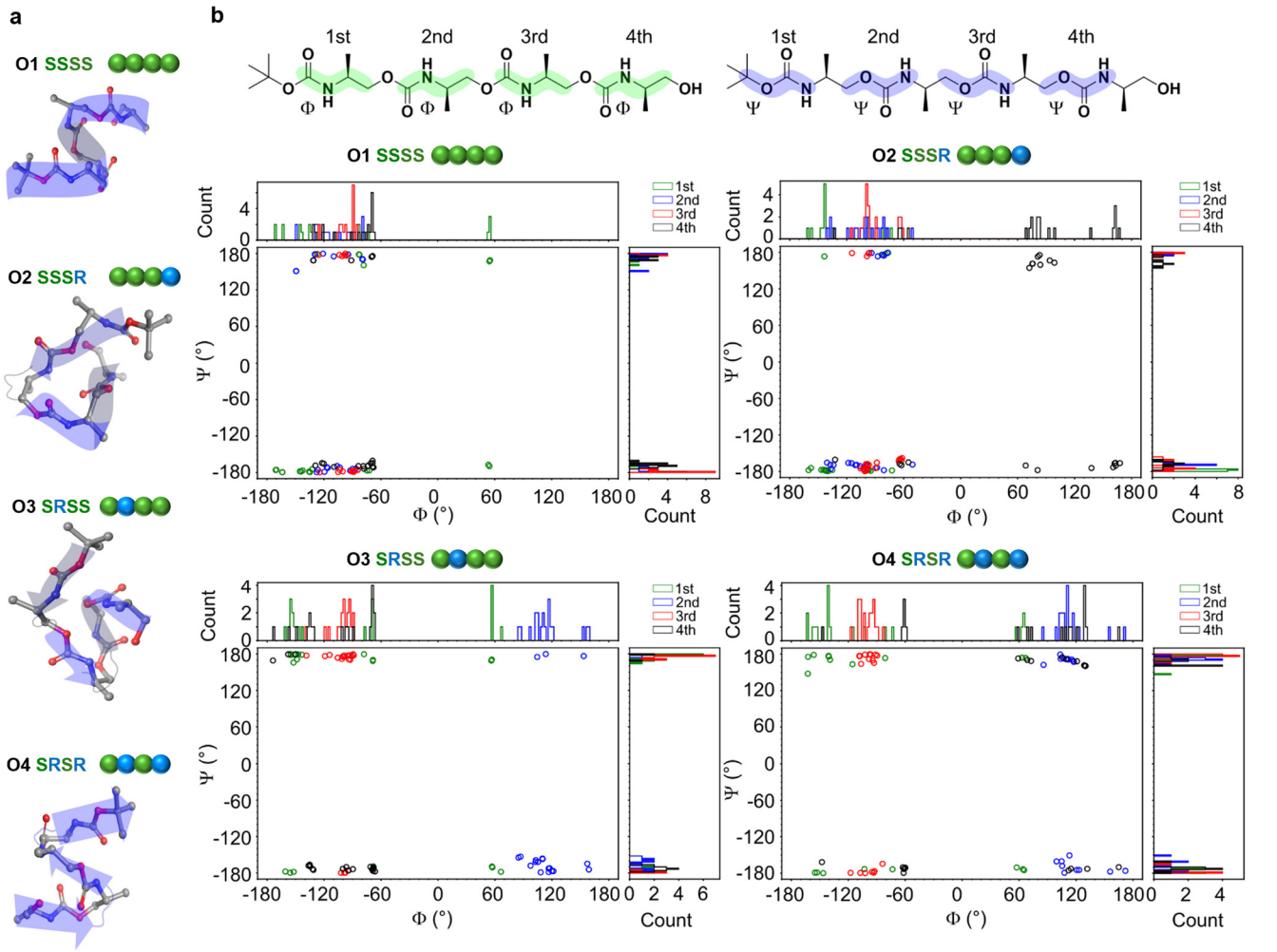

Fig. 3 Stereocontrol dictates oligourethane shapes. (a) Simulated structures of the lowest energy conformation of oligourethanes O1–O4 after a prior optimization of the initial structure geometries. (b) Ramachandran plot (dihedral angles Φ and Ψ) of oligourethanes O1–O4, with O1 and O4 representing helix and zig-zag, respectively.

elongated, displaying a rather zig-zag shape. The other oligomers represent intermediate structures. The **O2** ***SSSR*** and **O3** ***SRSS*** show a part of the chain forming a helical pattern, but flipping the chirality of one unit certainly introduces structural change. For all oligomers O1–O4, we observed a large energy gap (~1.5–2 kcal mol^{-1}) between the lowest energy conformations and the other conformers as indicated by Gibbs free energy (ΔG) analyses (Fig. S34). This is a stark contrast to the previous study on the Boc-S monomer, where six conformations were found within a 1 kcal mol^{-1} energy window.[44] Boc-S refers to *tert*-butyl (*S*)-(1-hydroxypropan-2-yl)(methyl)carbamate, which serves as the monomeric building block used for the synthesis of the oligomers O1–O4. The structural stability of oligomers is attributed to intramolecular hydrogen bonding between urethane units (C═O···H–N) as visualized by Non-Covalent Interaction (NCI) analyses for the lowest energy conformer of each tetramer (Fig. S35).

Stereocontrol tunes the geometry of oligomers by affecting intramolecular hydrogen bonds that guide torsions toward distinct angle preferences. The unique structural feature of urethanes is that the angle Ψ takes values only around −180, 0, 180°, meaning that the urethane bond is planar, as visualized in Fig. 3b.[44] The planarization is attributed to the extended delocalization of π-electrons. The most significant effect of the stereochemistry appears for Φ angles. The Φ angles for **O1** ***SSSS*** are mainly distributed between −60 and −180° (Fig. 3b, top left). When the stereocenters are altered, the majority of Φ angles flip the value signs. For sequence **O4** ***SRSR***, the Φ distribution of the first and third unit populates between −60 and −180° while the second and fourth unit populates between 60 and 180° (Fig. 3b, bottom right). The same tendency was observed for O2 and O3 oligomers (Fig. 3 top right and bottom left). This result suggests that stereochemistry can be used to design the folding structure of oligourethanes by dictating the sign of the torsion angle Φ. This is crucial information for the future programming of sequence-defined polyurethanes, where we could possibly control the polymer folding into a helix, sheet, coil *etc.*, through sequences of stereocenters.

Experimental investigation of oligourethane conformations in solution by spectroscopic analyses

Detailed experimental characteristics in non-aqueous media indicate that the secondary structure of oligourethanes is indeed dependent on stereochemistry, which proves the outcome of the computational data shown in Fig. 3a. Notably, while structural studies are commonly conducted in aqueous environments, our study was performed in chloroform, offering new insights into folding under non-aqueous conditions. Based on Nuclear Magnetic Resonance (NMR, Fig. 4 and S38–S41), Infrared (IR, Fig. 5a and S42) and Vibrational Circular Dichroism (VCD, Fig. 5b and S43) spectroscopies, we qualitatively characterized the formed shapes of the oligourethanes. The combination of NMR, IR, and VCD spectra has been used as a powerful method for studying molecular conformations of various systems[46–55] and has proved its relevance in analyzing the secondary structure of oligourethanes.

NMR reveals the structural differences between oligourethanes O1–O4 caused by the alteration in the sequence of stereocenters. In the ^{1}H NMR spectra the signals from methylene (CH_2) and methine (CH) groups in the backbone (range around 3.3–4.5 ppm) serve as distinctive fingerprints for a given oligomer (Fig. 4a). Concomitantly, a large variation of the peaks representing amine (NH) protons (around 4.5–6.8 ppm) is observed between four tetramers. These spectral differences are attributed to the various proton spatial arrangements that depend on the sequence among diastereoisomers. Similarly to ^{1}H NMR data the ^{13}C NMR spectra also show differences in chemical shift signals between stereosequence arrangements (Fig. S25–S28). At 300 K (about room temperature), all NMR signals are broadened, reflecting restricted molecular motions and limited rotational freedom of the oligourethanes. Heating up to 323 K does not cause a significant difference. In contrast, cooling reduces conformational exchange, moving the system out of the intermediate exchange regime, which sharpens and resolves the signals when the temperature reaches 263 K (Fig. 4b and Fig. S38a–41a). This effect likely arises from structured regions, such as folded helical segments, that create an anisotropic environment and increase spectral resolution. The presence of hydrogen bonds is confirmed by the characteristic downfield shift of

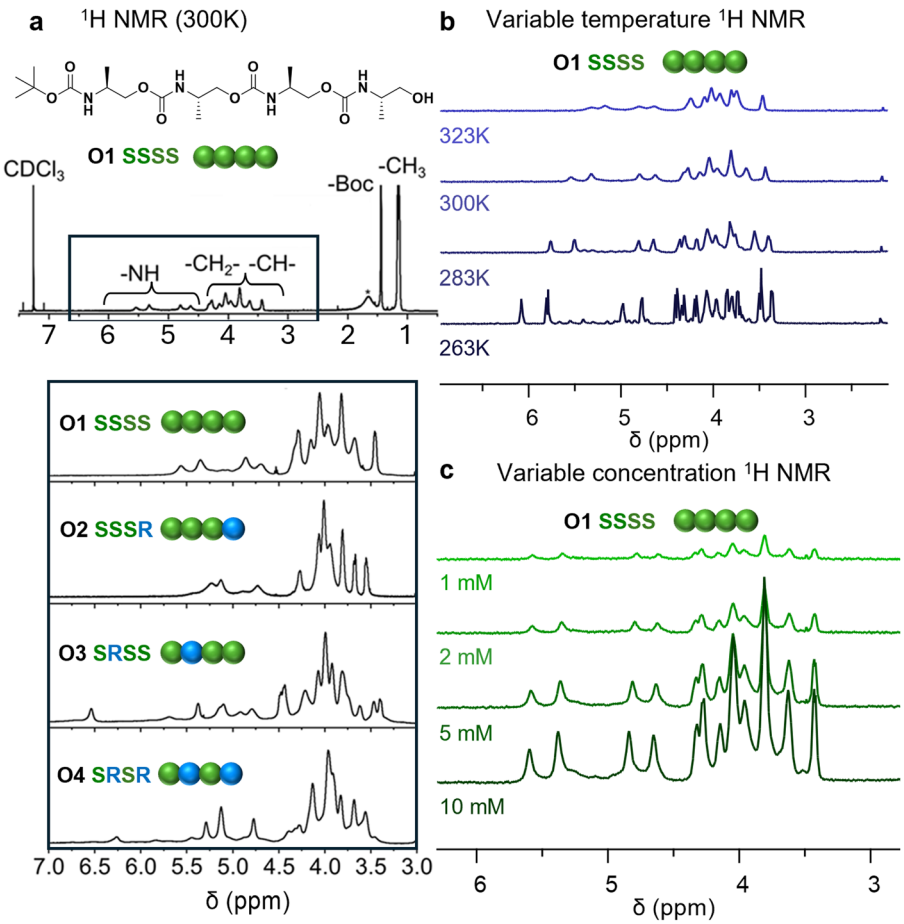

Fig. 4 Conformational variations caused by the sequence of stereocenters probed by ^{1}H NMR. (a) Full range ^{1}H NMR with signals assigned to corresponding functional groups (top) and zoomed range of amine and backbone protons (O1–O4, 5 mM). Amine and backbone protons reveal distinct signal patterns for each diastereoisomer, evidencing a particular spatial arrangement for each oligourethane tetramer. (b) Variable temperature ^{1}H NMR of **O1** ***SSSS*** oligourethane. (c) Variable concentration ^{1}H NMR of **O1** ***SSSS*** oligourethane.

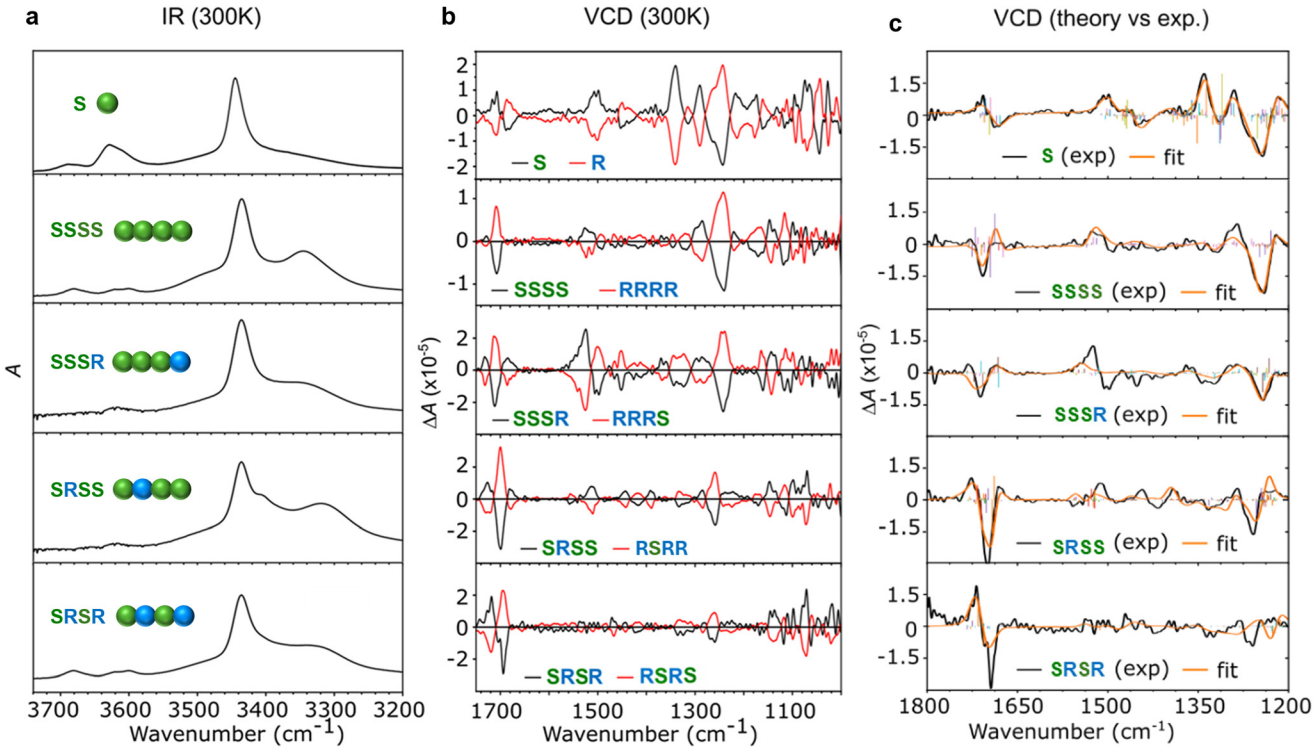

Fig. 5 Conformational variations caused by the sequence of stereocenters probed by IR and VCD spectroscopies in $CDCl_3$. (a) IR spectra range from 3200–3750 cm^{-1}, demonstrating differences in signal patterns between Boc-S (100 mM) monomer and oligourethane diastereoisomers (O1–O4, 15 mM). (b) VCD spectra of Boc-S monomer, oligourethanes (O1–O4, black) and their enantiomers (O1′–O4′, red). (c) Experimental VCD spectra compared with the best-fitted weighted average of the DFT calculated spectra of conformers.

NH proton signals during variable temperature NMR experiments (Fig. 4b and Fig. S38a–41a). It is present for all studied oligourethanes O1–O4 and their enantiomers O1′–O4′. The NMR analyses indicate significant spectral differences among O1–O4 are due to distinct intramolecular interactions and a formed hydrogen bond network. Variable-concentration ^1H NMR experiments in $CDCl_3$ in the concentration range 1–10 mM show no change in NH chemical shifts, confirming their intramolecular origin (Fig. 4c and Fig. S38b–41b).

Similarly, IR analyses of the four oligourethanes exhibit notable differences depending on the sequence of stereocenters, especially in the spectral range of 3200–3750 cm^{-1} representing NH stretching (Fig. 5a, full spectra Fig. S42). The broad peak around 3350 cm^{-1} in the oligomer spectra is assigned to hydrogen-bonded N–H, as the spectrum of Boc-S alone does not reveal this signal. When the stereocenter of the second unit is altered (**O3** ***SRSS***), a new peak appears at ~3400 cm^{-1}, and the broad band at ~3350 cm^{-1} shifts to ~3300 cm^{-1} compared to **O1** ***SSSS*** and **O2** ***SSSR***. Those results confirm that altering stereochemistry changes the environment of the hydrogen-bonded NH stretching mode along with NMR data.

In the VCD spectra, fingerprint regions (amide I, II and III) become indicative for assigning helical, zig-zag and disordered intermediate structures, similar to the amide range used for structural analysis of peptides.[56] A striking contrast emerges when comparing oligomer spectra to the monomer, highlighting the structural diversity driven by their 3D conformations. The VCD spectra of O1–O3 show qualitatively comparable signatures, while O4 reveals a clearly distinct spectral pattern. This aligns with the simulated conformations, which showed an ordered helix for O1, while flipping the chirality of one of the repeating units introduced disorder in helical structures of O2–O3. On the other hand, the VCD spectrum of O4 is different from O1–O3, which presumably reflects its elongated zig-zag sheet-like structure, further reinforcing the unique folding behavior of the studied sequences. The mirror-image relationship between the VCD spectra of enantiomeric pairs confirms the enantiopurity of the synthesized compounds (Fig. 5b). The experimental VCD spectrum of each sequence is statistically different as indicated by the cosine similarity analysis (Table S6). VCD spectra of the 20 lowest energy conformers were calculated using DFT employing B3LYP-D3/6-311++G(d,p)/PCM for each sequence (see SI for details). Using these 20 spectra as basis spectra, we performed linear combination fitting on the experimental spectrum (Fig. 5c). The fitting results showed that the most weighted conformers were not necessarily the lowest energy conformers (Tables S7–10). This is due to the challenge of DFT calculations in accurately determining the free energy of each conformer.[57] Nevertheless, it is remarkable that the experimental spectrum can be reproduced by the spectra of the 20 lowest energy conformers with

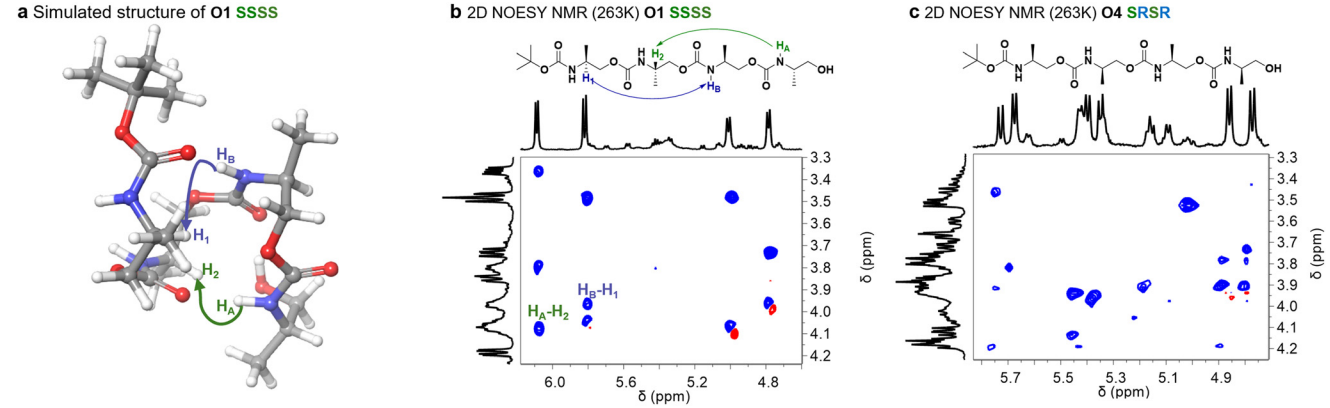

Fig. 6 (a) Simulated structure of **O1** ***SSSS*** illustrating characteristic through-space interactions for helical structure. (b) 2D NOESY NMR spectra (zoom of NH range) of **O1** ***SSSS*** in $CDCl_3$ (5 mM) with marked through-space interactions characteristic of helical secondary structure; other signals present in the spectra are attributed to TOCSY artifacts. The presence of observed cross signals serves as a confirmation of the helix model, which is in alignment with the findings discussed above. (c) 2D NOESY NMR spectra (zoom of NH range) of **O4** ***SRSR*** in $CDCl_3$ (5 mM) showing the lack of characteristic through-space interactions present in **O1** ***SSSS***. The observed cross signals in NOESY spectra are TOCSY artifacts. The multiple NH signals present in the spectra confirm the presence of multiple conformers.

good agreement. We also note that the structural features of the 20 lowest-energy conformers are similar within each sequence (Tables S7–10).

The 3D structural characterization of oligourethanes confirmed that the sequence of stereocenters guides the folding and conformation of oligourethanes to form helices, as indicated by computational studies. The helical structure of O1 oligourethane was confirmed by 2D Nuclear Overhauser Effect Spectroscopy (NOESY), detecting through-space proton interactions characteristic of oligourethane helical conformations (Fig. 6a and S57). To assign particular signals in ^{1}H NMR spectra, which is critical for structural analysis, we performed COSY (Fig. S45–S48) and TOCSY (Fig. S49–S52) analyses of all studied sequences O1–O4. Based on these spectral data, we identify individual spin systems representing each monomer unit, using a similar strategy as we reported previously for isotactic oligourethane (Fig. S53–S56).[58] The NOESY spectra show different signal patterns between diastereoisomers (Fig. S57–S60) that confirm their distinct spatial arrangements. Presented in Fig. 6b, the 2D NOESY spectrum of O1 shows characteristic NOE couplings between the amine and methine protons (NH_A-H_2 and NH_B-H_1) that match the DFT simulated structure. The same strategy was applied to analyze spectra of other oligomers (O2–O4). However, due to spectral complexity and signal overlapping caused by the disorder introduced as the effect of stereocenter alterations, it was not feasible to assign individual protons accurately, which is crucial for further structural analysis (for details see SI, Fig. S53–S56). As an example, the corresponding NOESY spectra of **O4** ***SRSR*** oligourethane are shown in Fig. 6c. For the oligourethane with an alternating sequence of stereocenters **O4** ***SRSR***, we do not observe NOESY cross-peaks characteristic of a helically folded structure. Instead, the absence of these signals may support the existence of an elongated, zig-zag-like conformation, where the increased distance between NH protons and backbone signals between the monomers prevents observation of cross-peaks typical of a compact, helically folded shape.

Conclusions

The sequence of stereocenters in the oligourethane backbone leads to various structural patterns in organic solvents, such as helical and sheet-like motifs, as evidenced by the range of methods, including NMR, IR, and VCD. The data show that stereochemistry can be used to design the folded structure of oligourethanes by dictating the sign of torsional angle values. An isotactic sequence (*SSSS*) forms a helical structure, whereas a syndiotactic sequence (*SRSR*) attains an elongated zig-zag resembling sheet-like structure. These examples prove that the secondary structure of sequence-defined oligomers can be tuned by stereochemistry. Our findings represent a significant step toward achieving precise control over the folding of oligo/polyurethanes in non-aqueous environments—an underexplored area, which opens up the possibility of engineering their shape and function. Therefore, stereocontrol is expected to play a crucial role in developing sequence-defined polymers as abiotic protein-like materials tailored for non-physiological environments, paving the way for unforeseen applications in organic-phase catalysis, chemical sensing, and interactive materials.

Author contributions

RS envisioned the initial design of sequence-defined polymers and the project goal. All the authors contributed to the detailed design of the project. SN and SGG synthesized and characterized oligomers (SEC, LC-MS, DSC, NMR). WD acquired the crystal structure of the **O3** ***SRSS*** oligomer. CB

acquired the crystal structure of the **O4 *SRSR*** oligomer. AFPM and JB performed IR and VCD experiments, as well as simulation and data analysis. The manuscript was written with contributions from all authors. All authors have approved the final version of the manuscript.

Conflicts of interest

The authors declare no competing financial interest.

Data availability

The data supporting this article manuscript have been included as part of the supplementary information (SI). Supplementary information: detailed description of the experimental procedures, including materials and methods, as well as additional data supporting the findings of this manuscript: LC-MS, SEC, IR, VCD, DFT, NMR, and X-ray. See DOI: https://doi.org/10.1039/d6py00299d.

CCDC 2454372 (**O3 *SRSS***) and 2454850 (**O4 *SRSR***) contain the supplementary crystallographic data for this paper.[59a,b]

Acknowledgements

RS, SN, and SGG thank the Polish National Science Centre (No 2018/31/D/ST5/01365, No 2021/43/I/ST4/01294) for financial support. We thank Katarzyna Chomiak (DSC), Janusz Skonieczny (NMR), and Katarzyna Kapczyńska (LC-MS) from Łukasiewicz-PORT for technical support during analyses. We are grateful to Katarzyna Slepokura from the Chemistry Faculty of Wroclaw University for access to crystallography analysis and support during data analysis. AFPM, JB, TB, and TBMA thank the University of Geneva for the financial support. TBMA thanks the partial financial support from the Swiss National Science Foundation (project grant SNSF 200021E_209555). CB thanks the Dubochet Center for Imaging (DCI) Geneva for the acquisition of the 3D electron diffraction structure.

References

1 J.-F. Lutz, J.-M. Lehn, E. W. Meijer and K. Matyjaszewski, From Precision Polymers to Complex Materials and Systems, *Nat. Rev. Mater.*, 2016, **1**(5), 16024, DOI: 10.1038/natrevmats.2016.24.
2 M. J. Austin and A. M. Rosales, Tunable Biomaterials from Synthetic, Sequence-Controlled Polymers, *Biomater. Sci.*, 2019, **7**(2), 490–505, DOI: 10.1039/C8BM01215F.
3 J. Lutz, Defining the Field of Sequence–Controlled Polymers, *Macromol. Rapid Commun.*, 2017, **38**(24), 1700582, DOI: 10.1002/marc.201700582.
4 J.-F. Lutz, M. Ouchi, D. R. Liu and M. Sawamoto, Sequence-Controlled Polymers, *Science*, 2013, **341**(6146), 1238149, DOI: 10.1126/science.1238149.
5 A. J. DeStefano, R. A. Segalman and E. C. Davidson, Where Biology and Traditional Polymers Meet: The Potential of Associating Sequence-Defined Polymers for Materials Science, *JACS Au*, 2021, **1**(10), 1556–1571, DOI: 10.1021/jacsau.1c00297.
6 R. Szweda, Sequence- and Stereo-Defined Macromolecules: Properties and Emerging Functionalities, *Prog. Polym. Sci.*, 2023, **145**, 101737, DOI: 10.1016/j.progpolymsci.2023.101737.
7 C. Mertens, M. Soete, M. L. Ślęczkowski, A. R. A. Palmans, E. W. Meijer, N. Badi and F. E. Du Prez, Stereocontrolled, Multi-Functional Sequence-Defined Oligomers through Automated Synthesis, *Polym. Chem.*, 2020, **11**(26), 4271–4280, DOI: 10.1039/D0PY00645A.
8 J. Li, M. Leclercq, M. Fossepré, M. Surin, K. Glinel, A. M. Jonas and A. E. Fernandes, Discrete Multifunctional Sequence-Defined Oligomers with Controlled Chirality, *Polym. Chem.*, 2020, **11**(24), 4040–4046, DOI: 10.1039/D0PY00537A.
9 J. C. Barnes, D. J. C. Ehrlich, A. X. Gao, F. A. Leibfarth, Y. Jiang, E. Zhou, T. F. Jamison and J. A. Johnson, Iterative Exponential Growth of Stereo- and Sequence-Controlled Polymers, *Nat. Chem.*, 2015, **7**(10), 810–815, DOI: 10.1038/nchem.2346.
10 X. Wang, X. Zhang, Y. Sun and S. Ding, Stereocontrolled Sequence-Defined Oligotriazoles through Metal-Free Elongation Strategies, *Macromolecules*, 2021, **54**(20), 9437–9444, DOI: 10.1021/acs.macromol.1c01371.
11 W. He, S. Wang, M. Li, X. Wang and Y. Tao, Iterative Synthesis of Stereo– and Sequence–Defined Polymers *via* Acid–Orthogonal Deprotection Chemistry, *Angew. Chem., Int. Ed.*, 2022, **61**(9), e202112439, DOI: 10.1002/anie.202112439.
12 J. M. Lee, J. Kwon, S. J. Lee, H. Jang, D. Kim, J. Song and K. T. Kim, Semiautomated Synthesis of Sequence-Defined Polymers for Information Storage, *Sci. Adv.*, 2022, **8**(10), eabl8614, DOI: 10.1126/sciadv.abl8614.
13 P. Cwynar, P. Pasikowski and R. Szweda, One-Pot Approach for Multi-Step, Iterative Synthesis of Sequence-Defined Oligocarbamates, *Eur. Polym. J.*, 2023, **182**, 111706, DOI: 10.1016/j.eurpolymj.2022.111706.
14 W. Forysiak, S. Kozub, Ł. John and R. Szweda, Discrete Oligourethanes of Sequence-Regulated Properties – Impact of Stereocontrol, *Polym. Chem.*, 2022, **13**(20), 2980–2987, DOI: 10.1039/D2PY00299J.
15 P. J. Flory, *Principles of Polymer Chemistry; The George Fisher Baker non-resident lectureship in chemistry at Cornell university*, Cornell university press, Ithaca (N.Y.) London, 1995.
16 A. M. Hanlon, C. K. Lyon and E. B. Berda, What Is Next in Single-Chain Nanoparticles?, *Macromolecules*, 2016, **49**(1), 2–14, DOI: 10.1021/acs.macromol.5b01456.
17 O. Altintas and C. Barner-Kowollik, Single–Chain Folding of Synthetic Polymers: A Critical Update, *Macromol. Rapid*

Commun., 2016, **37**(1), 29–46, DOI: 10.1002/marc.201500547.

18 T. Terashima, T. Mes, T. F. A. De Greef, M. A. J. Gillissen, P. Besenius, A. R. A. Palmans and E. W. Meijer, Single-Chain Folding of Polymers for Catalytic Systems in Water, *J. Am. Chem. Soc.*, 2011, **133**(13), 4742–4745, DOI: 10.1021/ja2004494.

19 G. Yilmaz, V. Uzunova, R. Napier and C. R. Becer, Single-Chain Glycopolymer Folding via Host–Guest Interactions and Its Unprecedented Effect on DC-SIGN Binding, *Biomacromolecules*, 2018, **19**(7), 3040–3047, DOI: 10.1021/acs.biomac.8b00600.

20 Y. Vo, R. Raveendran, C. Cao, R. Y. Lai, M. Lossa, H. Foster and M. H. Stenzel, Solvent Choice during Flow Assembly of Photocross-Linked Single-Chain Nanoparticles and Micelles Affects Cellular Uptake, *ACS Appl. Mater. Interfaces*, 2024, **16**(44), 59833–59848, DOI: 10.1021/acsami.4c12186.

21 Z. Han, Z. Li, M. H. Stenzel and R. Chapman, Collapsed Star Copolymers Exhibiting Near Perfect Mimicry of the Therapeutic Protein "TRAIL", *J. Am. Chem. Soc.*, 2024, **146**(31), 22093–22102, DOI: 10.1021/jacs.4c08658.

22 A. J. DeStefano, S. D. Mengel, M. W. Bates, S. Jiao, M. S. Shell, S. Han and R. A. Segalman, Control over Conformational Landscapes of Polypeptoids by Monomer Sequence Patterning, *Macromolecules*, 2024, **57**(4), 1469–1477, DOI: 10.1021/acs.macromol.3c02338.

23 M. A. Reith, S. Kardas, C. Mertens, M. Fossépré, M. Surin, J. Steinkoenig and F. E. Du Prez, Using, Nickel to Fold Discrete Synthetic Macromolecules into Single-Chain Nanoparticles, *Polym. Chem.*, 2021, **12**(34), 4924–4933, DOI: 10.1039/D1PY00229E.

24 S. H. Gellman, Foldamers: A Manifesto, *Acc. Chem. Res.*, 1998, **31**(4), 173–180, DOI: 10.1021/ar960298r.

25 C. M. Goodman, S. Choi, S. Shandler and W. F. DeGrado, Foldamers as Versatile Frameworks for the Design and Evolution of Function, *Nat. Chem. Biol.*, 2007, **3**(5), 252–262, DOI: 10.1038/nchembio876.

26 A. M. Rosales, R. A. Segalman and R. N. Zuckermann, Polypeptoids: A Model System to Study the Effect of Monomer Sequence on Polymer Properties and Self-Assembly, *Soft Mat.*, 2013, **9**(35), 8400, DOI: 10.1039/c3sm51421h.

27 P. Sang and J. Cai, Unnatural Helical Peptidic Foldamers as Protein Segment Mimics, *Chem. Soc. Rev.*, 2023, **52**(15), 4843–4877, DOI: 10.1039/D2CS00395C.

28 D. J. Hill, M. J. Mio, R. B. Prince, T. S. Hughes and J. S. Moore, A Field Guide to Foldamers, *Chem. Rev.*, 2001, **101**(12), 3893–4012, DOI: 10.1021/cr990120t.

29 S. Wang, L. Allmendinger and I. Huc, Abiotic Foldamer Quaternary Structures, *Angew. Chem., Int. Ed.*, 2024, **63**(48), e202413252, DOI: 10.1002/anie.202413252.

30 R. Kudirka, H. Tran, B. Sanii, K. T. Nam, P. H. Choi, N. Venkateswaran, R. Chen, S. Whitelam and R. N. Zuckermann, Folding of a Single–chain, Information–rich Polypeptoid Sequence into a Highly Ordered Nanosheet, *Biopolymers*, 2011, **96**(5), 586–595, DOI: 10.1002/bip.21590.

31 E. J. Robertson, A. Battigelli, C. Proulx, R. V. Mannige, T. K. Haxton, L. Yun, S. Whitelam and R. N. Zuckermann, Design, Synthesis, Assembly, and Engineering of Peptoid Nanosheets, *Acc. Chem. Res.*, 2016, **49**(3), 379–389, DOI: 10.1021/acs.accounts.5b00439.

32 D. Bécart, V. Diemer, A. Salaün, M. Oiarbide, Y. R. Nelli, B. Kauffmann, L. Fischer, C. Palomo and G. Guichard, Helical Oligourea Foldamers as Powerful Hydrogen Bonding Catalysts for Enantioselective C–C Bond-Forming Reactions, *J. Am. Chem. Soc.*, 2017, **139**(36), 12524–12532, DOI: 10.1021/jacs.7b05802.

33 S. Kohmoto, H. Takeichi, K. Kishikawa, H. Masu and I. Azumaya, Conformation of S-Shaped Aromatic Imide Foldamers and Their Induced Circular Dichroism, *Tetrahedron Lett.*, 2008, **49**(7), 1223–1227, DOI: 10.1016/j.tetlet.2007.12.034.

34 Z. Luo, N. Zhu and D. Zhao, Helical Folding Competing with Unfolded Aggregation in Phenylene Ethynylene Foldamers, *Chem. – Eur. J.*, 2016, **22**(31), 11028–11034, DOI: 10.1002/chem.201601804.

35 Z. C. Girvin and S. H. Gellman, Foldamer Catalysis, *J. Am. Chem. Soc.*, 2020, **142**(41), 17211–17223, DOI: 10.1021/jacs.0c07347.

36 I. Huc, S. Kwon and H. Lee, Synthetic Foldamers: Rational Design of Advanced Structures with Diverse Applications, *ChemPlusChem*, 2021, **86**(8), 1042–1043, DOI: 10.1002/cplu.202100288.

37 P. Prabhakaran, G. Priya and G. J. Sanjayan, Foldamers: They're Not Just for Biomedical Applications Anymore, *Angew. Chem., Int. Ed.*, 2012, **51**(17), 4006–4008, DOI: 10.1002/anie.201107521.

38 S. Kwon, V. Morozov, L. Wang, P. K. Mandal, S. Chaignepain, C. Douat and I. Huc, Interrogating the Potential of Helical Aromatic Foldamers for Protein Recognition, *Org. Biomol. Chem.*, 2024, **22**(48), 9342–9347, DOI: 10.1039/D4OB01436G.

39 D. Deepak, J. Wu, V. Corvaglia, L. Allmendinger, M. Scheckenbach, P. Tinnefeld and I. Huc, DNA Mimic Foldamer Recognition of a Chromosomal Protein, *Angew. Chem., Int. Ed.*, 2025, **64**(8), e202422958, DOI: 10.1002/anie.202422958.

40 R. Gopalakrishnan, A. I. Frolov, L. Knerr, W. J. Drury and E. Valeur, Therapeutic Potential of Foldamers: From Chemical Biology Tools To Drug Candidates?, *J. Med. Chem.*, 2016, **59**(21), 9599–9621, DOI: 10.1021/acs.jmedchem.6b00376.

41 A. Sharma, P. Cwynar, A. Jose, V. Gupta and R. Szweda, Step-Economy Approach for Scalable Synthesis of Stereocontrolled and Sequence-Defined Polyurethanes, *Eur. Polym. J.*, 2025, **236**, 114120, DOI: 10.1016/j.eurpolymj.2025.114120.

42 U. S. Gunay, B. E. Petit, D. Karamessini, A. Al Ouahabi, J.-A. Amalian, C. Chendo, M. Bouquey, D. Gigmes, L. Charles and J.-F. Lutz, Chemoselective Synthesis of Uniform Sequence-Coded Polyurethanes and Their Use as Molecular Tags, *Chem*, 2016, **1**(1), 114–126, DOI: 10.1016/j.chempr.2016.06.006.

43 W. Forysiak, A. Lizak and R. Szweda, Sequence of Monomers and Position of Stereocenters Matter for Thermal Properties of Stereocontrolled Oligourethanes, *ChemPhysChem*, 2024, **25**(17), e202400366, DOI: 10.1002/cphc.202400366.

44 A. F. Perez Mellor, J. Brazard, S. Kozub, T. Bürgi, R. Szweda and T. B. M. Adachi, Unveiling the Configurational Landscape of Carbamate: Paving the Way for Designing Functional Sequence-Defined Polymers, *J. Phys. Chem. A*, 2023, **127**(35), 7309–7322, DOI: 10.1021/acs.jpca.3c02442.

45 M. Szatko, W. Forysiak, S. Kozub, T. Andruniów and R. Szweda, Revealing the Effect of Stereocontrol on Intermolecular Interactions between Abiotic, Sequence-Defined Polyurethanes and a Ligand, *ACS Biomater. Sci. Eng.*, 2024, **10**(6), 3727–3738, DOI: 10.1021/acsbiomaterials.4c00456.

46 C. Merten, Recent Advances in the Application of Vibrational Circular Dichroism Spectroscopy for the Characterization of Asymmetric Catalysts, *Eur. J. Org. Chem.*, 2020, (37), 5892–5900, DOI: 10.1002/ejoc.202000876.

47 S. Knoppe and T. Bürgi, Chirality in Thiolate-Protected Gold Clusters, *Acc. Chem. Res.*, 2014, **47**(4), 1318–1326, DOI: 10.1021/ar400295d.

48 A. Pérez-Mellor, I. Alata, V. Lepère and A. Zehnacker, Conformational Study of the Jet-Cooled Diketopiperazine Peptide Cyclo Tyrosyl-Prolyl, *J. Phys. Chem. B*, 2019, **123**(28), 6023–6033, DOI: 10.1021/acs.jpcb.9b04529.

49 L. A. Nafie, Vibrational Optical Activity: From Discovery and Development to Future Challenges, *Chirality*, 2020, **32**(5), 667–692, DOI: 10.1002/chir.23191.

50 K. D. R. Eikås, M. T. P. Beerepoot and K. Ruud, A Computational Protocol for Vibrational Circular Dichroism Spectra of Cyclic Oligopeptides, *J. Phys. Chem. A*, 2022, **126**(32), 5458–5471, DOI: 10.1021/acs.jpca.2c02953.

51 T. B. Freedman, X. Cao, R. K. Dukor and L. A. Nafie, Absolute Configuration Determination of Chiral Molecules in the Solution State Using Vibrational Circular Dichroism, *Chirality*, 2003, **15**(9), 743–758, DOI: 10.1002/chir.10287.

52 T. A. Keiderling, Protein and Peptide Secondary Structure and Conformational Determination with Vibrational Circular Dichroism, *Curr. Opin. Chem. Biol.*, 2002, **6**(5), 682–688, DOI: 10.1016/S1367-5931(02)00369-1.

53 K. J. Jalkanen, M. Elstner and S. Suhai, Amino Acids and Small Peptides as Building Blocks for Proteins: Comparative Theoretical and Spectroscopic Studies, *J. Mol. Struct. THEOCHEM*, 2004, **675**(1–3), 61–77, DOI: 10.1016/j.theochem.2003.12.045.

54 C. Gautier and T. Bürgi, Chiral Gold Nanoparticles, *ChemPhysChem*, 2009, **10**(3), 483–492, DOI: 10.1002/cphc.200800709.

55 A. Pérez-Mellor, I. Alata, V. Lepere and A. Zehnacker, Chirality Effects in the Structures of Jet-Cooled Bichromophoric Dipeptides, *J. Mol. Spectrosc.*, 2018, **349**, 71–84, DOI: 10.1016/j.jms.2018.02.005.

56 T. A. Keiderling, Structure of Condensed Phase Peptides: Insights from Vibrational Circular Dichroism and Raman Optical Activity Techniques, *Chem. Rev.*, 2020, **120**(7), 3381–3419, DOI: 10.1021/acs.chemrev.9b00636.

57 G. Marton, M. A. J. Koenis, H.-B. Liu, C. A. Bewley, W. J. Buma and V. P. Nicu, Titelbild: An Artificial Intelligence Approach for Tackling Conformational Energy Uncertainties in Chiroptical Spectroscopies (Angew. Chem. 38/2023), *Angew. Chem.*, 2023, **135**(38), e202310358, DOI: 10.1002/ange.202310358.

58 M. Szatko, R. Konefał, S. Njoku, K. Zwoliński, T. Andruniów and R. Szweda, Solvent Effect on Secondary Structures of Discrete, Isotactic, Oligourethane Motif – towards Engineering Protein-like Features in Abiotic Polymers, *Eur. Polym. J.*, 2025, 114262, DOI: 10.1016/j.eurpolymj.2025.114262.

59 (*a*) CCDC 2454372: Experimental Crystal Structure Determination, 2026, DOI: 10.5517/ccdc.csd.cc2ncz9b; (*b*) CCDC 2454850: Experimental Crystal Structure Determination, 2026, DOI: 10.5517/ccdc.csd.cc2ndgq8.